N94-22305

Lidar and Radar derived Cirrus Microphysical Properties for the 26 November 1991 Case Study

Janet M. Intrieri and Graham Feingold

Cooperative Institute for Research in Environmental Sciences
University of Colorado/NOAA
Campus Box 449
Boulder, Colorado 80309-0449

1. Cirrus Parameters from Combined Lidar and Radar Measurements

The Wave Propagation Laboratory's CO_2 lidar ($\lambda = 10.6\ \mu m$) and Ka-band radar ($\lambda = 8.66$ mm) operate at widely separated wavelengths; the differences in how the transmitted waves interact with cloud targets can be exploited to provide information that neither sensor could provide alone. This can be as simple as overlapping the data sets to provide additional coverage on cloud geometry (see Uttal and Intrieri, 1993) or combining the measurements in a theoretical framework to provide cirrus cloud parameters of the size spectrum, i.e., characteristic particle size and number concentration. In this paper, the latter option is described and an example case study presented to illustrate the types of information available for cloud and radiation transfer models.

The wavelength-dependent difference in returned backscatter from the same-sized particle forms the theoretical basis of the lidar-radar method (Intrieri et al., 1993). This particular combination of wavelengths provides information on particle sizes as shown in Fig. 1a where the slope in the ratio of lidar to radar backscatter Kernels indicates unambiguous information throughout the spectrum of most cloud particle sizes. The predicted sizes are constrained by the lower limit sensitivity of the radar (making $\sim 30\ \mu m$ the smallest predictable characteristic size) and attenuation from particles by the lidar (usually from clouds having an optical depth greater than 2). Corrections for attenuation and specular reflection are made to the lidar signal as needed. The error in predicted size increases as the theoretical curves become flat with increasing size (see Fig. 1b, solid line). However, the effective radii inferred from our data thus far have not been larger than $\sim 225\ \mu m$, which fall well within reasonable size ranges for cirrus clouds. Because the lidar and radar produce range-resolved information, size estimates can be determined every 75 m throughout the depth of the cloud. This allows us to analyze the microphysical evolution of the cloud (i.e., growth, decay, precipitation, etc.) along with the changing radiation fields.

Once r_e is determined, the number densities (N_o) can be calculated from either the radar or lidar backscatter. A similar method was used for determining size distribution information from dual polarization radar (e.g. Feingold and Levin, 1987). In Fig. 1b the theoretical curve used to estimate the number density from the radar backscatter is also plotted (dashed line).

Using the derived r_e and N_o, the ice water content (*iwc*) of the cirrus clouds can be calculated using

$$iwc = 4/3\pi\rho\int r^3 n(r)dr = 4/3\pi\rho N_o 3/8 r_e^3, \qquad (1)$$

where $n(r)$ is the size distribution of ice particles and ρ is the density of ice, assumed to be 0.9 g cm^{-3}. Figure 2 shows the radii having the largest contributions to η (radar backscatter coefficient), β (lidar relative backscatter), and *iwc* (respectively r_η, r_β, and r_i) as a function of the mode radius of $n(r)$. Essentially, r_β, r_i, r_η are the 2nd, 3rd, and 6th moment weighted mode radii. We see that $r_\beta < r_i < r_\eta$ illustrating the added value of using the lidar data in combination with the radar data, versus using the radar information alone, to infer ice water contents in cirrus clouds because the correlation between r_β and r_i is better than that between r_η and r_i.

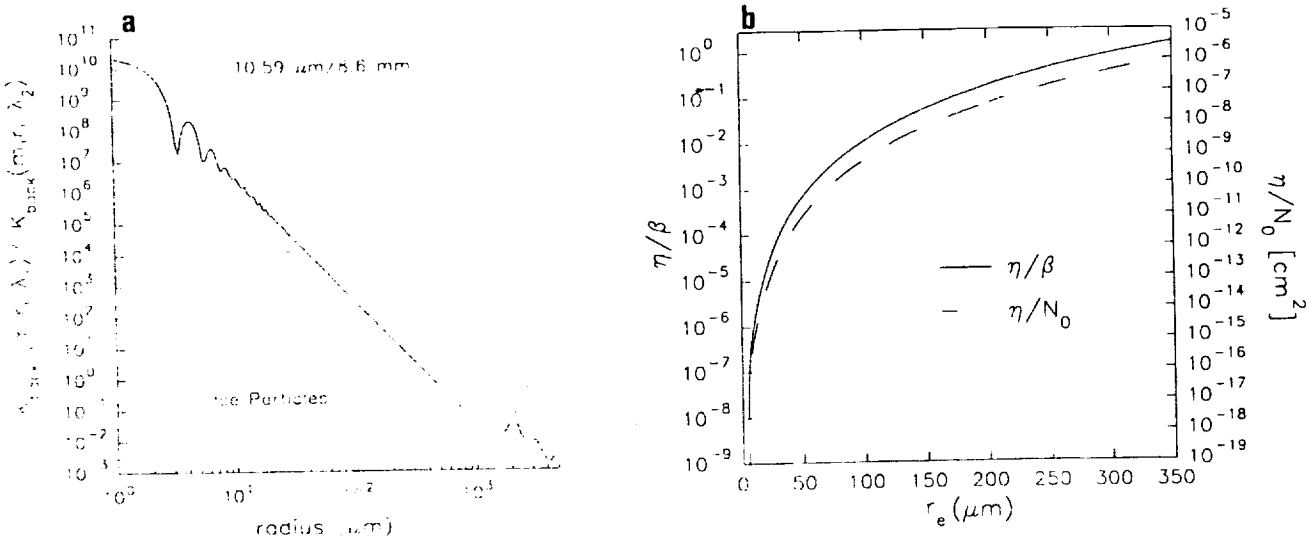

Fig. 1. a) Ratio of lidar to radar Kernels as a function of particle size. b) Theoretical curves of radar/lidar backscatter coefficients, η/β, (solid line) and radar backscatter/number density, η/N_o, (dashed line) vs. effective radius, μm.

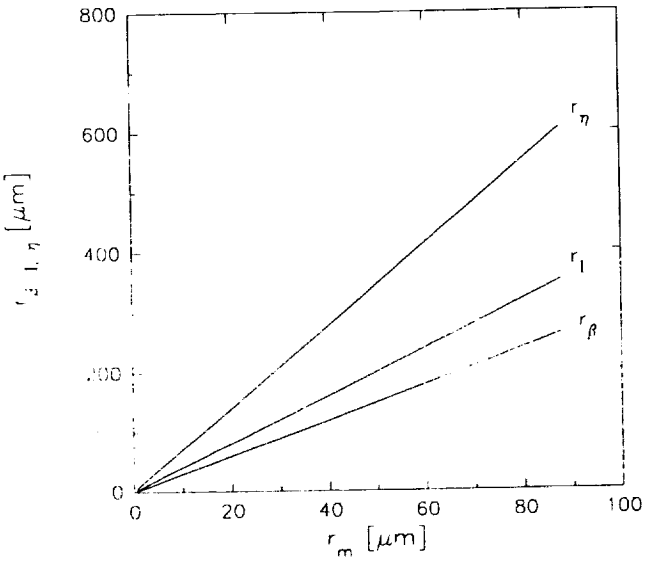

Fig. 2. The 2nd, 3rd, and 6th moment weighted mode radii (r_β, r_l, r_η, respectively) as a function of the mode radius r_m.

2. Cirrus Cloud Case Study

On 26 November 1991 a cirrus cloud system exhibiting three phases was observed passing overhead by the radar and lidar over a period of 5.5 h. During phase 1 the cirrus cloud was thin and tenuous and was detected only by the lidar (1600-1730 UTC, 9-10 km AGL). During phase 2 the cirrus cloud deepened (8-10 km AGL) and similar boundaries were detected by both the lidar and radar (1730-1900 UTC). Later, in phase 3, the cloud became optically thick enough to sporadically attenuate the lidar signal (1900-2130 UTC). The time-height cross sections of r_e, N_o, and *iwc* for the period from 1737-1855 UTC are presented in Fig. 3.

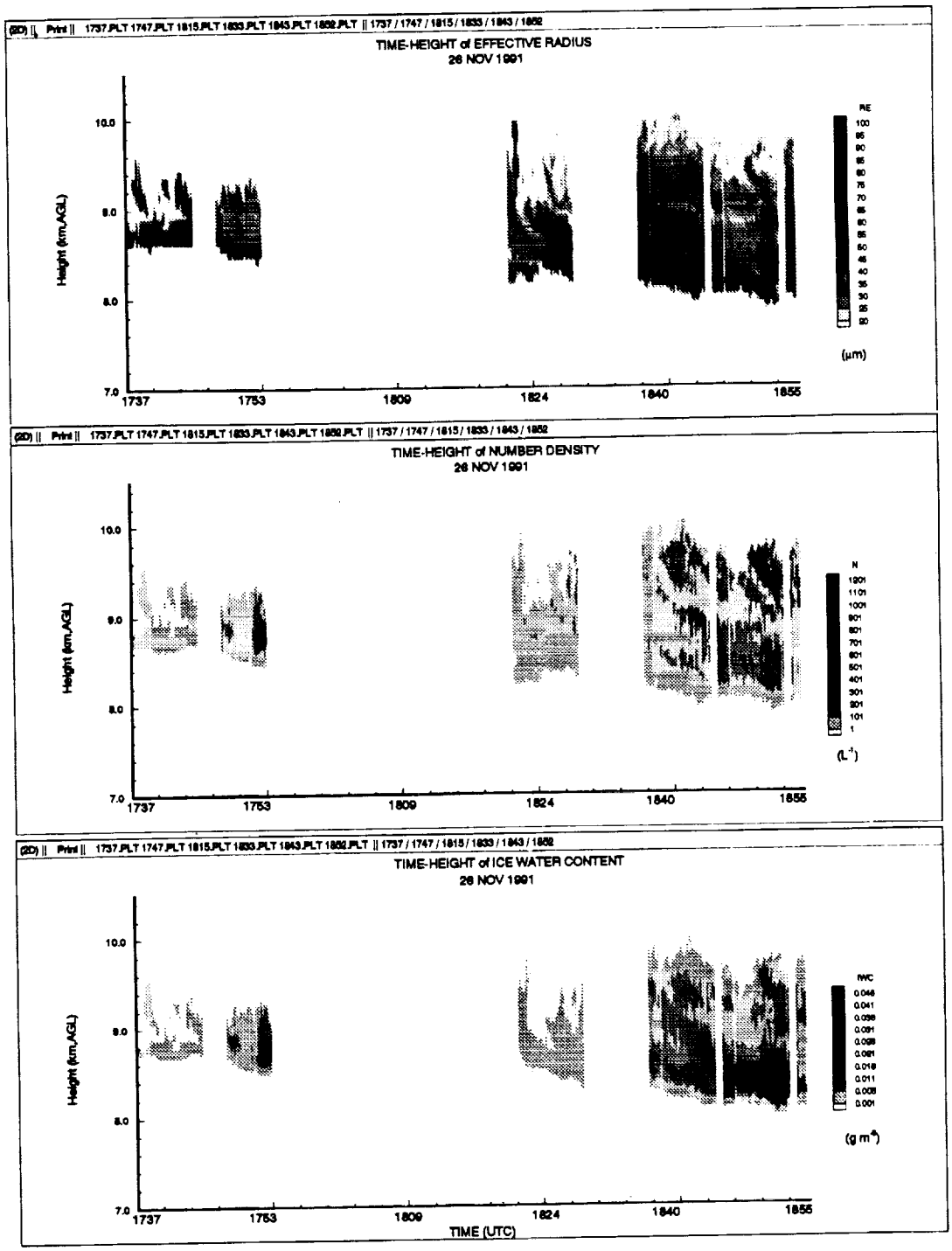

Fig. 3. Time-height series of a) effective radius (μm), b) number density (l^{-1}), and c) ice water content (g m^{-3}) from 1737 to 1855 UTC on 26 November 1991.

In Figure 3a, the effective radii, in μm, are plotted. Note that the largest effective radii are located at the cloud bottom, in banded structures within the cloud, and in the turret-like feature at 1820 UTC. Particles having the smallest r_e are located in other regions within the cloud and at the top of cloud from 1840-1855 UTC. The number densities, in l^{-1}, (Fig. 3b) tend to be a maximum in location above the maximum in

r_e and are often better correlated with the *iwc* field (Fig. 3c). For example, the large concentration of small particles in the upper regions of the cloud at 1850 UTC suggests a nucleation region. The *iwc* profiles, in g m^{-3}, indicate that the cloud from 1820 to 1830 UTC is emitting less IR radiation downward than the cloud from 1845 to 1855 UTC (Fig. 3c).

3. Summary

By utilizing multiple-sensor combinations and integrating data sets we can begin to understand how thickness, size distribution and optical properties affect cirrus cloud radiative properties. An important advantage of using the radar and lidar is that they can obtain extended periods of measurements with good spatial and temporal resolution, whereas aircraft, the primary alternative for cloud sampling, are expensive and limited to only a few hours of data sampled one point at a time. Combined lidar and radar cloud information can be obtained from 3 s which is appropriate for smaller scale cloud microphysical or radiation models.

Much needed longer term cloud statistics can be easily compiled (i.e., cloud boundaries, particle sizes, and number concentration) for larger scale models needing average bulk property parameterizations. This information can be reduced to any time increment from 3 s to as long as the data was obtained i.e. 1 month of wintertime continental cirrus.

Acknowledgements. The authors would like to thank everyone who operated and maintained the lidar and radar during the FIRE II experiment. This work was supported by a grant titled Cloud Remote Sensing in National Climate Research Programs, from NOAA's Climate and Global Change Program Office.

References

Feingold, G. and Z. Levin, 1987: Application of the lognormal raindrop distribution to differential reflectivity radar measurements (Z_{DR}). *J. Atmos. Oceanic Tech.*, 4, 377-382.

Intrieri, J.M., G.L. Stephens, W.L. Eberhard, and T. Uttal, 1993: A method for determining cirrus cloud particle sizes using a lidar/radar backscatter technique. *J. Appl. Meteor.*, 32, 1074-1082.

Uttal, T., and J.M. Intrieri, 1993: Comparison of cloud boundaries measured with 8.6 mm radar and 10.6 μm lidar (This volume).